

# Structural Behaviour of Superconducting H<sub>3</sub>S at Megabar Pressure

P. Modak\* and A. K. Verma

High Pressure & Synchrotron Radiation Physics Division  
Bhabha Atomic Research Centre, Mumbai-400085, India

## Abstract

A new era has begun in the field of superconductivity with the discovery of phonon mediated superconductivity at 203 K in the compressed hydrogen disulfide (H<sub>2</sub>S) gas. A series of studies has attributed the observed superconductivity to a compound H<sub>3</sub>S that results from the decomposition of compressed H<sub>2</sub>S at high pressures. The superconducting properties of conventional superconductors can be computed precisely once the underlying microscopic crystal structure is fully known. In this work using evolutionary crystal structure searches in combination with first-principles calculations, we predict a new metallic phase of H<sub>3</sub>S in the pressure interval of 108-166 GPa. The novelty of new phase is that it consists of SH<sub>6</sub>, SH<sub>3</sub> and S units that results both cationic and anionic charge state for S and H atoms. Our work shows that the high-T<sub>c</sub> explanations based on structures reported earlier may not be adequate and thus more work is needed for arriving at a precise understanding of the observed high-T<sub>c</sub> in this material.

**Keywords:** Phonon mediated superconductivity, Metallic phase, crystal orbital Hamiltonian population (COHP)

## Introduction

Superconductivity the phenomenon of non-resistive conduction of electricity below critical temperature (T<sub>c</sub>) remains one of the hot topics in the material science. It was first discovered by H. K. Onnes in Hg at 4.2 K in 1911. Over the years several new superconductors were identified leading to the discovery of 18 K superconductivity in Nb<sub>3</sub>Sn in 1954 [1]. However, the ultimate goal of achieving a room temperature superconductor is still a distant dream though a T<sub>c</sub> of 133 K has been achieved in the Hg based cuprates at ambient pressure that increases to 164 K at 30 GPa [2, 3]. The prospect of getting higher T<sub>c</sub> in this family of compounds is not clear as the nature of superconductivity is still not fully understood. In contrast, the Bardeen-Cooper-Schrieffer (BCS) formalism provides a clear guide to achieve high T<sub>c</sub>; all that needed is a favourable combination of high frequency phonons, strong electron-phonon coupling and high electronic density of states at the Fermi level. Based on the BCS formalism, it was predicted that under the application of pressures of the order of 25 GPa, Hydrogen would exhibit superconductivity at high

temperature [4, 5]. However the metallization of hydrogen is a challenging problem in the high pressure research to date. Formation of metallic atomic hydrogen at high pressure has been difficult to establish in diamond-anvil cells. There have been claims on experimental evidence for a metallic phase at pressures,

from 250 GPa to 495 GPa [6-8], but the findings of these works have not yet been unambiguously accepted by the scientific community [6-10]. Ashcroft [11] proposed that the metallization pressure for hydrogen could be lowered by chemical pre-compression or via doping. Driven by this idea, there is a surge in the high pressure research activities on the hydrogen rich solids in recent years [12-14].

One of the remarkable successes of these efforts is the observation of a record breaking 203 K superconductivity in the compressed H<sub>2</sub>S gas announced in the year 2015 [15]. Though the T<sub>c</sub> is well below the room temperature, this discovery is considered to be a definitive forward step towards the realisation of a room temperature superconductor. However the composition and crystal structure of superconducting phase have not been well characterized, as it is observed that compressed H<sub>2</sub>S molecules dissociate under high pressure (above 27 GPa and at 300 K) [16]. A large number of

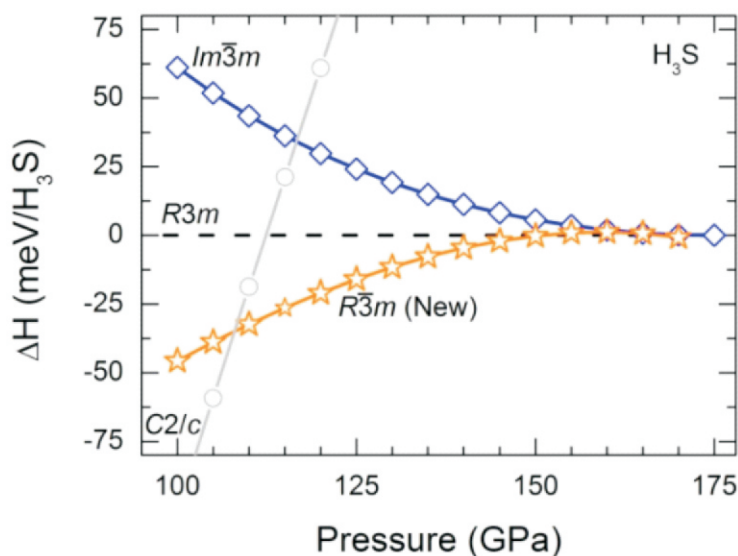
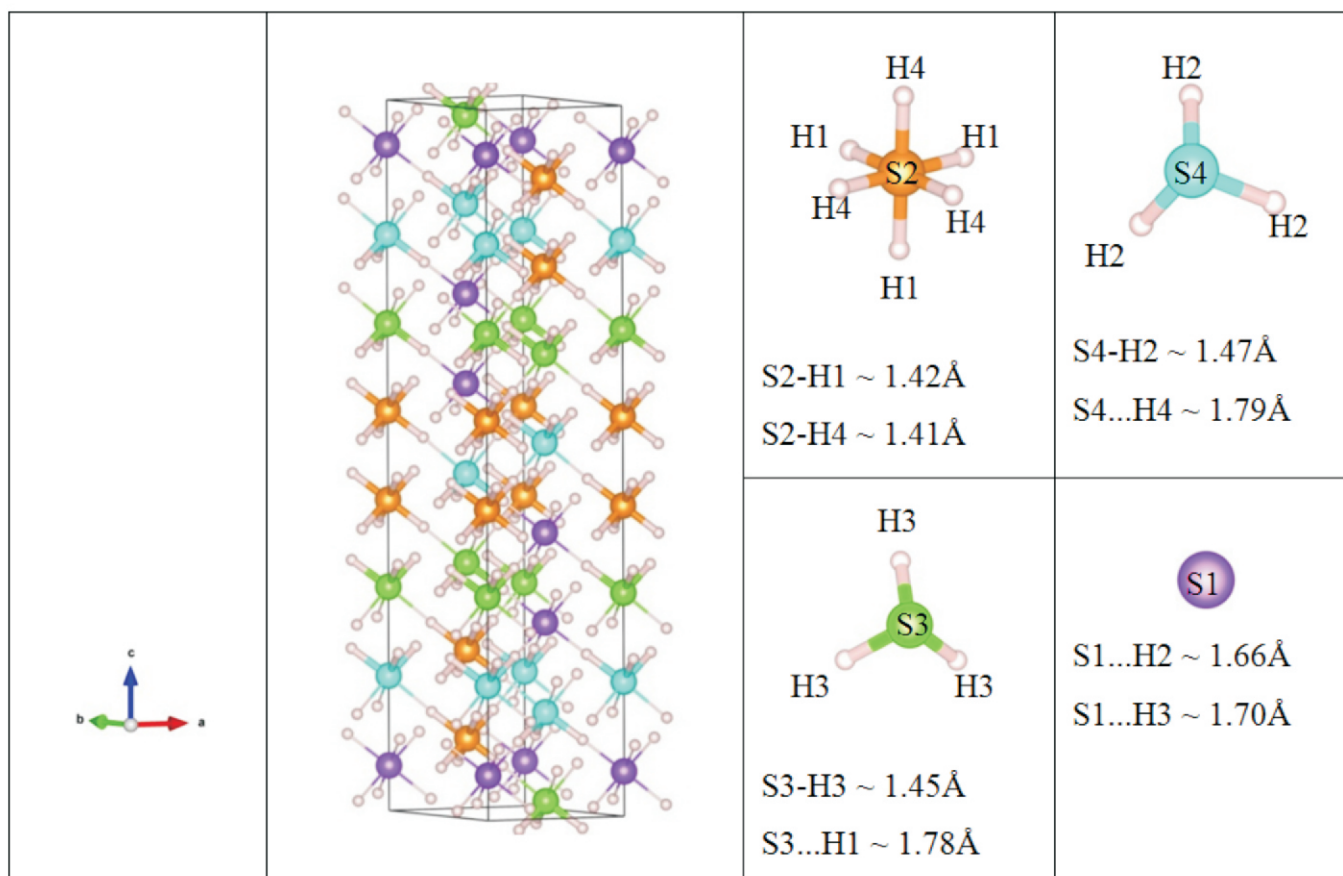


Fig. 1: Pressure variation of enthalpy for the most important structures of H<sub>3</sub>S. Here enthalpies are estimated relative to known R3m structure (Ref. 23).



**Fig. 2:** Ball-and-stick model of the newly predicted trigonal structure ( $R\bar{3}m$ ,  $Z=24$ ) of  $H_3S$ . Here, S-H covalent bonds are shown by thick rods and S...H hydrogen bonds are shown by thin rods. Bond-lengths are given at 110 GPa (Ref. 23).

investigations, on the high pressure behaviour of H-S system, have commenced immediately after this discovery [17-19]. A consensus about decomposition of  $H_2S$  and formation of new compounds under high pressure emerged based on consistent results reported from several experimental and theoretical studies [18-19]. It is widely believed that the formation of  $H_3S$  compound is responsible for the high  $T_c$  superconductivity in compressed  $H_2S$ . Recent high pressure experiments with  $H_2+S$  sample reports formation of  $H_3S$  compound above 70 GPa [20].

There are reports on the high pressure phase diagram of  $H_3S$  compound based on first principle studies [17, 21]. It is predicted that  $H_3S$  metalizes at 112 GPa in trigonal structure ( $R\bar{3}m$ ,  $Z=3$ ); further compression would result in a phase transition to cubic bcc structure ( $Im\bar{3}m$ ,  $Z=2$ ) around 175 GPa [17]. Few other non-metallic  $H_3S$  structures, orthorhombic ( $Cccm$ ,  $Z = 16$ , 37-112 GPa), monoclinic ( $C2/c$ ,  $Z = 16$ , 2-112 GPa) and triclinic  $P1$  ( $Z=8$ , 0-37 GPa), were also proposed. Surprisingly lowest enthalpy non-metallic  $C2/c$  structure has not been observed in

any experiments but they observed orthorhombic  $Cccm$  structure [20, 22]. Hence the high pressure phase diagram of  $H_3S$  is still not well characterized even after various theoretical and experimental studies. Recently, we have carried out high pressure crystal structure searches using evolutionary algorithm combining with first-principles relaxations to unveil the high pressure phase diagram of  $H_3S$  [23]. Results are discussed in the light of the experimentally observed pressure dependence of the transition temperature  $T_c$ .

### Theoretical methods

Crystal structure searches were carried out using evolutionary algorithm as implemented in the USPEX code [24-26] and the first-principles calculations were carried out using VASP code [27-30]. In these calculations, we have used all-electron frozen-core projector-augmented wave (PAW) potentials and generalized-gradient approximation (GGA) for exchange-correlation energy. To understand bonding characteristics we have also calculated crystal orbital Hamiltonian population (COHP) using

TB-LMTO-ASA code [31].

### Results & Discussion

In low pressure region (<100 GPa) our crystal structure searches correctly reproduce all earlier known structures. Below 108 GPa, we find a monoclinic structure ( $C2/c$ ,  $Z = 16$ ) as the energetically most favourable structure. We also predict two new metastable structures namely; a monoclinic ( $C2/m$ ,  $Z = 16$ ) and a tetragonal structure ( $P4\bar{c}2$ ,  $Z = 8$ ) in this pressure region. We find that our proposed tetragonal  $P4\bar{c}2$  structure is energetically superior to the earlier proposed orthorhombic structure ( $Cccm$ ,  $Z = 16$ ). Further we noticed that orthorhombic  $Cccm$  structure relaxes to tetragonal  $P4\bar{c}2$  structure under full structural optimization at 75 GPa and above. Although  $C2/m$  and  $P4\bar{c}2$  structures do not have the lowest enthalpies but the possibility of their formation is not completely ruled out under favourable conditions of pressure and temperature.

Above 100 GPa our searches uncover a completely new trigonal structure ( $R\bar{3}m$ ,  $Z=24$ ) which is energetically superior to the earlier accepted trigonal

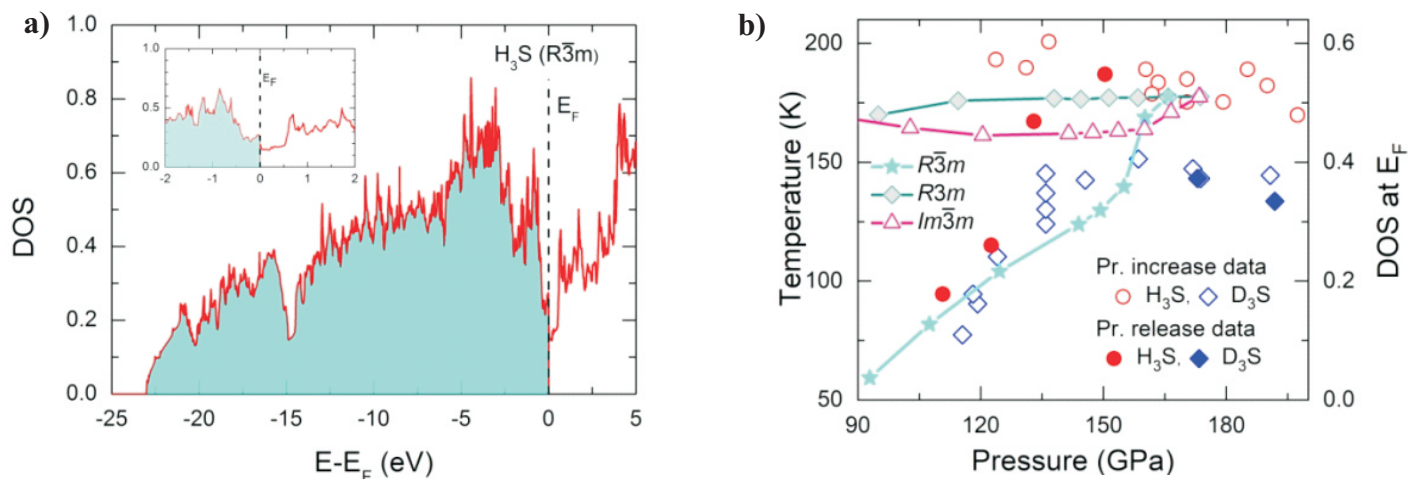


**Fig. 3: (a) Total Electronic DOS of  $R\bar{3}m$  phase of  $H_3S$  at 120 GPa. (b) Pressure variation of total DOS value at the Fermi-level. Here DOS is given in units of states/eV/ $H_3S$ . (Ref. 23).**

structure ( $R3m$ ,  $Z=3$ ). We find that the low pressure monoclinic  $C2/c$  structure makes a transition to our new structure at 108 GPa with a 6.25% volume reduction. On further compression  $R\bar{3}m$  structure transforms to a cubic structure ( $Im\bar{3}m$ ,  $Z=2$ ) at 166 GPa. Therefore the stability region of  $R\bar{3}m$  structure is 108-166 GPa (Fig.1). We also find that in the pressure range 150-166 GPa two trigonal structures coexist with very small differences in enthalpy (maximum enthalpies difference  $\sim 1.0$  meV/ $H_3S$ ). The dynamic stability of this new structure is established by calculating phonon spectrum that contains only real and positive frequencies.

Now to understand to what extent this newly found  $R\bar{3}m$  structure differs from earlier known  $R3m$  and  $Im\bar{3}m$  structures we carried out its structural analysis. We find that the new structure consists of  $SH_6$ ,  $SH_3$  and S units contrary to the  $R3m$  and  $Im\bar{3}m$  structures that consist of only  $SH_3$  and  $SH_6$ , respectively (Fig. 2). In all three structures the structural units are connected through S...H hydrogen-bonds. Presence of different structural units in the new structure leads to different local environments around S atoms that in turn results four different bond lengths both for S-H covalent and S...H hydrogen-bonds (Fig.2).

Our Bader charge analysis reveals different charge states for S and H atoms in different structural units of this structure. We find  $SH_6$  unit is very similar to  $SF_6$  molecule as in both units S has positive charge and H has negative charge like halide ions. But in the  $SH_3$  unit S has negative charge and H has

positive charge like alkali ions. Therefore both cationic and anionic charge states of H and S exist in new structure. We find that in  $R\bar{3}m$  structure pressure induced symmetrization of hydrogen-bonds take place at,  $\sim 166$  GPa where it makes a transition to a cubic  $Im\bar{3}m$  structure.

Our electronic structure analysis shows that three electronic bands cross the Fermi-level leading to one hole and two electron Fermi-sheets for new structure. We find that the total electronic DOS function is free electron like below to -20 eV, however close to the Fermi-level, on occupied side, there is a peak corresponding to van Hove singularity (VHS) and on other side there is a pseudo gap (Fig.3a). The van Hove singularity represents a critical point in the electronic density of state (DOS) function which induces electronic instabilities in the system. Generally, it has been seen that a VHS helps in formation of lower energy states like superconductivity. Pseudogap refers to a minimum in the electronic DOS function at the Fermi-level but in the context of superconductivity, especially in high-temperature superconductors; it refers to an energy range near the Fermi level which has very few states associated with it. Generally, pseudogaps forms when favourable electron-lattice interactions are present in the system. Underdoped cuprate superconductors are famous examples that exhibit pseudogaps above the transition temperature.

We find that close to the Fermi-level the DOS contributions come mainly from hydrogen  $1s$  and sulfur  $3p$  states. The S

atom present in  $SH_6$  structural unit contributes maximum to the DOS value at the Fermi-level. Compared to the old  $R3m$  structure, the total DOS value at Fermi-level for  $R\bar{3}m$  structure is considerably lower and it smoothly increases under pressure reaching to that of  $Im\bar{3}m$  structure near to 166 GPa. As electron-phonon coupling constant is directly proportional to DOS value at the Fermi-level, we expect lower electron-phonon coupling and consequently the lower  $T_c$  for  $R\bar{3}m$  structure below 155 GPa provided other parameters remain unaltered. Interestingly the pressure variation of DOS value at the Fermi-level behaves similar to the observed pressure variation of  $T_c$  (Fig.3b). It is worth mentioning that the Fermi-level DOS values of the earlier structures (i.e.,  $R3m$  and  $Im\bar{3}m$ ) do not exhibit such pressure behaviour, their Fermi-level DOS values remain nearly constant under pressure and hence they do not support the experimental observations.

Mechanism of superconductivity in compressed  $H_3S$  is widely believed to be of BCS type and the observation of strong isotope shift of  $T_c$  in deuterated samples further supports this view [15, 32]. The experimental value of the isotope coefficient ( $\alpha$ ) is  $\sim 0.3$ , at pressure above 170 GPa [15]. It is worthwhile to mention that the ideal BCS value of is 0.5. However deviations in  $\alpha$  values, from the 0.50, are a general feature of the BCS type superconductors. In recent years proposals of a non-BCS type of mechanism in  $H_3S$  are also put forward by some groups of researchers [33-35].

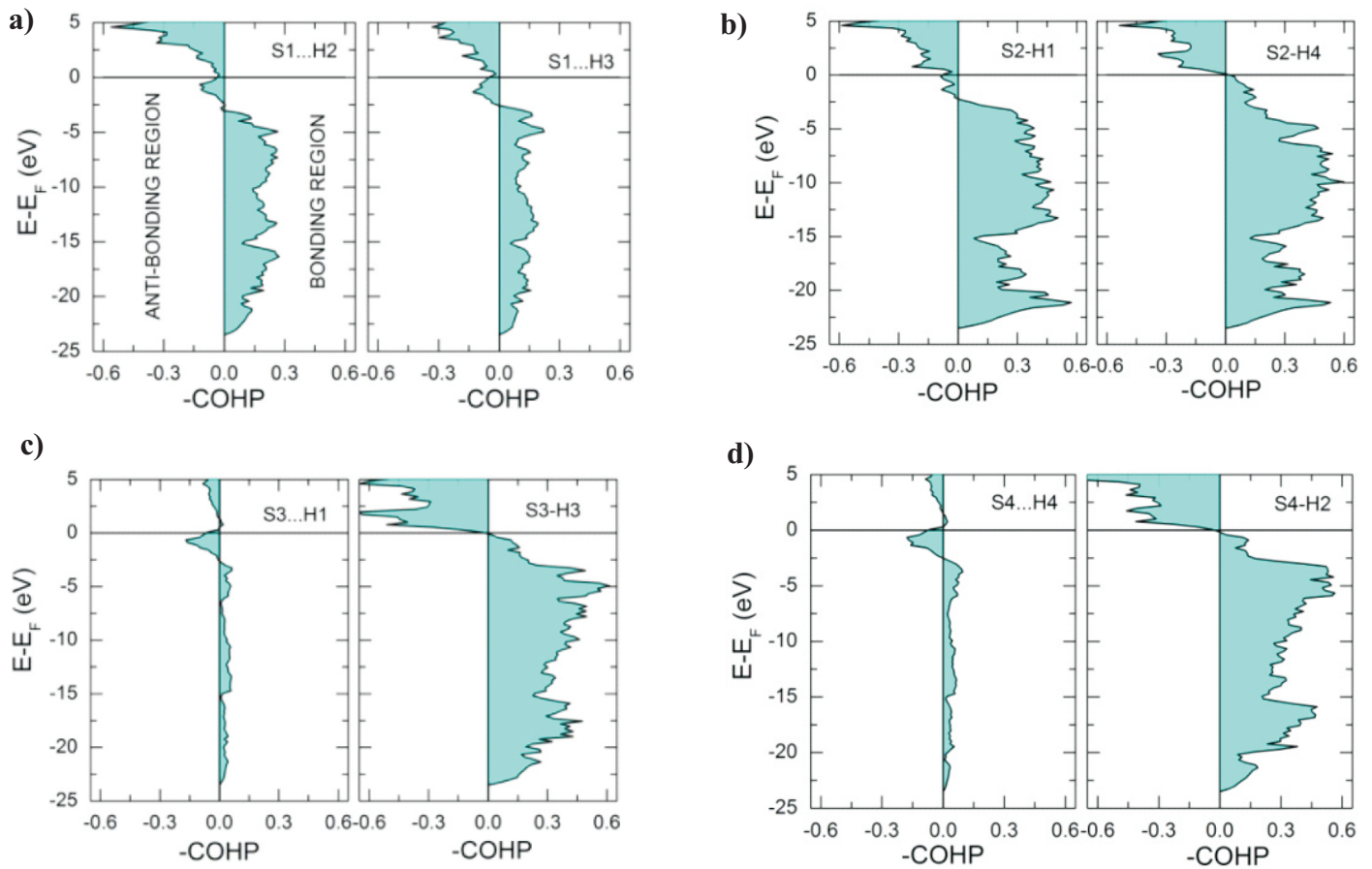


Fig. 4: The COHP functions of  $R\bar{3}m$  phase of  $H_3S$  at 120 GPa (Ref.23).

To understand the nature of S-H covalent bonds in different structural units, we have carried out crystal orbital Hamiltonian populations (COHP) analysis [36]. The COHP is an efficient tool to extract bonding information based on the electronic structure calculations. In a given energy window, its negative values describe bonding interactions and positive values describe anti-bonding interactions. It is customary to plot  $-COHP$  as a function of energy as shown in Fig.4 for different S-H pairs. Our analysis show that except S2-H1 covalent bond all other covalent bonds give bonding interactions as COHP is negative below Fermi-level. For  $R\bar{3}m$  and  $Im\bar{3}m$  structures, we find that the Fermi-level is located in the region of anti bonding states for S-H covalent bonds indicating an inherent instable nature of these structures. This also explains why  $R\bar{3}m$  structure is more stable compared to  $R\bar{3}m$  and  $Im\bar{3}m$  structures. We also find that S...H hydrogen bonds around S structural units have significant covalent character. COHP analysis also reveals that the S-H and B-B covalent bonds in  $MgB_2$  are different in character as the origin of metallicity of these two bonds is different.

## Conclusions

In summary, we have studied the structural behaviour of  $H_3S$  under high pressure using evolutionary crystal structure searches and first-principles calculations. Our searches unveiled a completely new structure in the trigonal crystal system over a large pressure interval ( $\sim 108$ -166 GPa). The newly proposed structure is metallic in nature and it consists of  $SH_6$ ,  $SH_3$  and S units that are connected through strong S...H hydrogen-bonds. In the  $SH_6$  unit, H is chemically halogen like whereas in  $SH_3$  units it behaves like alkali metal. At lower pressures new structure has smaller total electronic DOS at Fermi level in comparison to earlier structures hinting that earlier  $T_c$  estimations based on old structures may not be precise. Interestingly, for new structure pressure variation of total DOS values at the Fermi-level correlate well with the observed pressure variation of superconducting transition temperature that is absent for the earlier  $R\bar{3}m$  structure.

## Corresponding Author\*

P Modak (pmodak@barc.gov.in)

## References

- [1] B. Matthias, T. Geballe, S. Geller, and E. Corenzwit, Phys. Rev., **95**, 1435 (1954).
- [2] A. Schilling, M. Cantoni, J. D. Guo and H. R. Ott, Nature, **363**, 56 (1993).
- [3] L. Gao, Y. Y. Xue, F. Chen, Q. Xiong, R. L. Meng, D. Ramirez, C. W. Chu, J. H. Eggert, and H. K. Mao, Phys. Rev. B, **50**, 4260 (1994).
- [4] E. Wigner, and H. B. Huntington, J. Chem. Phys., **3**, 764–770 (1935).
- [5] N. W. Ashcroft, Phys. Rev. Lett., **21**, 1748–1749 (1968).
- [6] P. Loubeyre, F. Occelli and P. Dumas, Nature, **577**, 631 (2020).
- [7] M. Eremets, I. Troyan and A. P. Drozdov, arXiv: Materials Science (2016).
- [8] R. P. Dias and I. F. Silvera, Science, **355**, 715 (2017).

- [9] X.-D. Liu, P. Dalladay-Simpson, R.T. Howie, B. Li, and E. Gregoryanz, *Science*, **357**, eaan 2286 (2017).
- [10] A.F. Goncharov and V.V. Struzhkin, *Science*, **357**, eaan9736 (2017).
- [11] N. W. Ashcroft, *Phys. Rev. Lett.*, **92**, 187002 (2004).
- [12] M. Somayazulu, M. Ahart, A. K. Mishra, Z. M. Geballe, M. Baldini, Y. Meng, V.V. Struzhkin, and R. J. Hemley, *Phys. Rev. Lett.*, **122**, 027001 (2019).
- [13] A. P. Drozdov, P. P. Kong, V. S. Minkov, S. P. Besedin, M. A. Kuzovnikov, S. Moza\_ari, L. Balicas, F. Balakirev, D. Graf, V. B. Prakapenka, E. Greenberg, D. A. Knyazev, M. Tkacz, and M. I. Eremets, *Nature*, **569**, 528 (2019).
- [14] E. Snider, N. Dasenbrock-Gammon, R. McBride, M. Debessai, H. Vindana, K. Vencatasamy, K. V. Lawler, A. Salamat, and R. P. Dias, *Nature*, **586**, 373 (2020).
- [15] A. P. Drozdov, M. I. Eremets, I. A. Troyan, V. Ksenofontov, and S. I. Shylin, *Nature*, **525**, 73 (2015).
- [16] H. Fujihisa, H. Yamawaki, M. Sakashita, A. Nakayama, T. Yamada, and K. Aoki, *Phys. Rev. B*, **69**, 214102 (2004).
- [17] D. Duan, Y. Liu, F. Tian, D. Li, X. Huang, Z. Zhao, H. Yu, B. Liu, W. Tian, and T. Cui, *Sci. Rep.*, **4**, 6968 (2014).
- [18] N. Bernstein, C. S. Hellberg, M. D. Johannes, I. I. Mazin, and M. J. Mehl, *Phys. Rev. B*, **91**, 060511(R) (2015).
- [19] I. Errea, M. Calandra, C. J. Pickard, J. Nelson, R. J. Needs, Y. Li, H. Liu, Y. Zhang, Y. Ma, and F. Mauri, *Phys. Rev. Lett.*, **114**, 157004 (2015).
- [20] B. Guigue, A. Marizy and P. Loubeyre, *Phys. Rev. B*, **95**, 202104 (2017).
- [21] Y. Li, L. Wang, H. Liu, Y. Zhang, J. Hao, C. J. Pickard, J. R. Nelson, R. J. Needs, W. Li, Y. Huang, I. Errea, M. Calandra, F. Mauri, and Y. Ma, *Phys. Rev. B*, **93**, 020103(R) (2016).
- [22] A. F. Goncharov, S. S. Lobanov, I. Kruglov, X. M. Zhao, X. J. Chen, A. R. Oganov, Z. Konopkova and V. B. Prakapenka, *Phys. Rev. B*, **93**, 174105 (2016)
- [23] Ashok K. Verma and P. Modak, *Phys. Chem. Chem. Phys.*, **20**, 26344 (2018).
- [24] A.R. Oganov and C.W. Glass, *J. Chem. Phys.*, **124**, 244704 (2006).
- [25] A. O. Lyakhov, A.R. Oganov, H.T. Stokes, and Q. Zhu, *Comp. Phys. Comm.*, **184**, 1172 (2013).
- [26] A.R. Oganov, A.O. Lyakhov, and M. Valle, *Accounts of Chem. Research*, **44**, 227 (2011).
- [27] G. Kresse and J. Hafner, *J. Phys.: Condens. Matter*, **6**, 8245 (1994).
- [28] P. E. Blöchl, *Phys. Rev. B*, **50**, 17953 (1994).
- [29] G. Kresse, and J. Furthmüller, *Comput. Mater. Sci.*, **6**, 15 (1996).
- [30] G. Kresse, and D. Joubert, *Phys. Rev. B*, **59**, 1758 (1999).
- [31] O. K. Andersen, Stuttgart Tight-binding LMTO Program version 4.7, *Max Planck Institute Für Festkörperforschung*.
- [32] I. A. Troyan, et al., *Science* **351**, 1303–1306 (2016).
- [33] N. Bernstein, C. S. Hellberg, M. D. Johannes, I. I. Mazin, M. J. Mehl, *Phys. Rev. B* **91**, 060511 (2015).
- [34] S. Mozaffari et al., *Nature Communications* **10**, 2522 (2019).
- [35] E. F. Talantsev, *Supercond. Sci. Technol.* **33**, 124001 (2020).
- [36] R. Dronskowski, and P. E. Blöchl, *J. Phys. Chem.*, **97**, 8617 (1993).